J. Cell. Mol. Med. Vol 13, No 9B, 2009 pp. 3283-3295

Effect of genetic *SSTR4* ablation on inflammatory peptide and receptor expression in the non-inflamed and inflamed murine intestine

Joeri Van Op den bosch [a], Pascal Torfs [a], Benedicte Y. De Winter [b], Joris G. De Man [b], Paul A. Pelckmans [b], Eric Van Marck [c], David Grundy [d], Luc Van Nassauw [a, e], Jean-Pierre Timmermans [a, *]

[a] *Laboratory of Cell Biology & Histology, Department of Veterinary Sciences, University of Antwerp, Antwerpen, Belgium*
[b] *Laboratory of Experimental Medicine and Pediatrics, Division of Gastroenterology, Faculty of Medicine, University of Antwerp, Antwerpen, Belgium*
[c] *Laboratory of Pathology, Faculty of Medicine, University of Antwerp, Wilrijk, Belgium*
[d] *Department of Biomedical Science, University of Sheffield, Sheffield, UK*
[e] *Laboratory of Human Embryology & Anatomy, Faculty of Medicine, University of Antwerp, Antwerpen, Belgium*

Received: October 24, 2008; Accepted: March 6, 2009

Abstract

The recently suggested pivotal role of somatostatin (SOM) receptor 4 (SSTR4) in inflammation and nociception in several non-intestinal organs and in gastrointestinal (GI) physiology, necessitates exploration of the role of SSTR4 in GI pathophysiology. Therefore, the role of SSTR4 in GI activity was explored by investigating the effects of *SSTR4* deficiency on intestinal motility, smooth muscle contractility and on the expression of SSTRs and neuropeptides in the healthy and *Schistosoma mansoni*-infected murine small intestine. Functional experiments revealed no differences in intestinal motility or smooth muscle cell contractility between wild-type and SSTR4 knockout (*SSTR4*$^{-/-}$) mice in physiological conditions. As revealed by multiple immunofluorescent labellings, RT-PCR and quantitative real time RT-PCR (qPCR), genetic deficiency of SSTR4 considerably altered the expression of SOM and SSTRs in non-inflamed and inflamed conditions, affecting both extrinsic and intrinsic components of the intestinal innervation, along with SSTR expression in several non-neuronal cell types. Moreover, substance P and calcitonin gene-related peptide expression were significantly elevated in *SSTR4*$^{-/-}$ mice, confirming the modulatory role of SSTR4 on intestinal pro-inflammatory neuropeptide expression. These data suggest that SSTR4 plays a previously unexpected modulatory role in the regulation of intestinal SSTR expression. Moreover, in addition to the recently described inhibitory effects of SSTR4 on the neuronal release of pro-inflammatory peptides, SSTR4 appears also to be involved in the neuronal expression of both pro- and anti-inflammatory peptides in the murine small intestine.

Keywords: somatostatin • somatostatin receptor • inflammation • SSTR4 knockout mouse

Introduction

One of the peptidergic key players in the regulation of almost all aspects of gastrointestinal (GI) activity is somatostatin (SOM). Its effects are mediated by the G protein-coupled SOM receptors (SSTRs), five members of which have been characterized so far (SSTR1–SSTR5). All SSTR subtypes exist in a single protein isoform, except for SSTR2, which is alternatively spliced into a SSTR2A and a SSTR2B isoform. Although SSTR2 initially was believed to be the main SSTR subtype involved in SOM-mediated GI effects, recent data demonstrate that other SSTR subtypes are also involved [1–3]. The observation that SSTR1 and SSTR4, next to SSTR2, are also expressed in the murine ileum makes these two receptors valid candidates to mediate at least part of the SOM-dependent effects in the small intestine [1]. However, the potential role of these receptors in GI physiology remains to be elucidated.

SSTR4 recently gained attention as a crucial component in the inflammatory effects of SOM at different sites of inflammation.

*Correspondence to: Prof. dr. J.-P. TIMMERMANS,
Laboratory of Cell Biology & Histology,
Department of Veterinary Sciences, University of Antwerp,
Groenenborgerlaan 171, 2020 Antwerp, Belgium.
Tel.: 00323 265 33 00
Fax: 00323 265 33 01
E-mail: jean-pierre.timmermans@ua.ac.be

doi:10.1111/j.1582-4934.2009.00760.x

SOM-mediated inflammation-suppressive effects can be subdivided into two classes of action. The first one consists of the effects of SOM on inflammatory cells, either directly by targeting these cells or indirectly by modulating cells capable of synthesizing and releasing pro-inflammatory mediators. The best documented effects in this category include the somatostatinergic inhibition of lymphoid cell proliferation, cytokine and immunoglobulin production and the release of interferon-γ and of interleukins [4–7]. The second group of SOM-mediated anti-inflammatory actions is less well understood and includes suppression of the release of pro-inflammatory peptides from sensory nerve endings. During inflammation, pro-inflammatory mediators, mainly tachykinins (substance P and neurokinin A) and calcitonin gene-related peptide (CGRP), are released from capsaicin-sensitive sensory nerve endings, initiating an inflammatory cascade. In several non-intestinal tissues, the effects of these peptides are counteracted by SOM, released from nerve terminals of the same or distinct populations of primary afferent neurons [8, 9]. This neuronally released SOM exerts both a local, inhibitory effect on the release of the pro-inflammatory peptides substance P and CGRP, and a short-lasting systemic anti-inflammatory action *via* the systemic circulation [10]. Moreover, this locally released, neuronally derived SOM acts as a potent analgesic by inhibiting the excitability of peripheral nociceptors, including transient receptor potential vanilloid type 1 (TRPV1) [11–14].

In contrast to the direct effects of SOM on inflammatory cells, which probably involve all SSTR subtypes, the neurogenic inhibitory and analgesic effects of SOM seem to be primarily mediated by SSTR4 and, to a lesser extent, SSTR1. Recent pharmacological studies demonstrated the potency of SSTR4-selective agonists to reduce neurogenic and non-neurogenic inflammatory reactions in various animal models, whereas the mainly SSTR2-preferring SOM analogue octreotide had no effect [15–17]. In line with these results, we were recently able to demonstrate by means of immunohistochemistry the expression of SSTR4 in extrinsic afferent nerve fibres supplying the murine small intestine [1]. However, the specific functional role of this receptor in GI pathology remains to be investigated. The recent availability of *SSTR4*$^{-/-}$ mice opens up a unique opportunity to investigate the unexplored role of this receptor in GI activity, both in normal and in inflamed conditions. We therefore focussed on the expression of SOM, SSTRs and the pro-inflammatory neuropeptides substance P and CGRP in the small intestine of these knockout mice. Both the non-inflamed and the inflamed murine ileum were used to study the postulated crucial role of a SSTR4-mediated pathway in the anti-inflammatory actions of SOM in the GI tract (GIT). In line with our previous studies on the role of SOM and its receptors in GI pathophysiology, we used acutely *Schistosoma* (*S.*) *mansoni*-infected mice as a model for intestinal inflammation.

Moreover, as so far only the brain of *SSTR4* knockout mice has been studied, information on the effects of SSTR4 on the morphological and functional characteristics of the murine small intestine is completely lacking [18, 19]. Therefore, several functional and morphological features of the *SSTR4* knockout and wild-type (WT) ileum were compared in non-inflamed and inflamed conditions.

Methods

Animals

All studies were performed in adult C57Bl/6J *SSTR4* knockout/*lacZ* knockin mice (*SSTR4*$^{-/-}$, kindly provided by Dr. J.P. Allen and Dr. I.-S. Selmer) and congenic WT mice of both genders. *SSTR4*$^{-/-}$ and WT mice, aged 8 weeks, were infected with *S. mansoni* as described [20]. All experimental procedures were approved by the Medical Ethical Committee on Animal Experimentation of the University of Antwerp. Morphological and molecular biological data on the expression of SOM and SSTRs in non-inflamed and *S. mansoni*-infected WT ileum were published previously and will therefore not be repeated in detail [1]. As the measurement of *in vivo* motility, *in vitro* smooth muscle strip contractility, quantitative analyses on the density of enteric substance P-, CGRP- and SSTR1-expressing nerve fibres and quantitative real time RT-PCR (qPCR) experiments for substance P, CGRP-α and CGRP-β in WT ileum were not described earlier, these experimental data in WT and *SSTR4*$^{-/-}$ mice are reported in this paper.

In vivo measurement of gastrointestinal motility

GI motility was measured *in vivo* as previously described ($n = 8$ for both WT and *SSTR4*$^{-/-}$ mice) [21]. Briefly, mice, which were fasted for 18 hrs with free access to tap water, received an intragastric injection of 0.1 ml of a semiliquid non-nutrient dye (Evans blue 50 mg/ml dissolved in 0.5% methylcellulose). Fifteen minutes later the mice were anaesthetized, killed and the stomach and small intestine were carefully removed. *Small intestinal transit* was measured from the pylorus to the most distal point of migration of Evans blue and expressed as percent migration of Evans blue compared to the total length of the small intestine. Afterwards, the stomach was removed as one segment and the small intestine was divided into five equal segments. The stomach and the intestinal segments were put in 20 ml 0.1 N NaOH, minced and placed in an ultrasonic bath for 1 hr. The resulting suspension was left at room temperature for 1 hr. Five millilitres of the supernatant was then centrifuged at 1356 × *g* for 20 min. at 4°C. Samples were further diluted 1:5 in 0.1N NaOH and absorbance of the samples was measured spectrophotometrically at a wavelength of 565 nm (A_{565}). The *geometric centre* of the GI transit, which is considered the standard in quantifying distributional changes in transit of marker, was calculated using the following equation: $GC = \Sigma(\%A_{565}$ of Evans blue per segment × segment number)/100.

In vitro measurement of gastrointestinal contractility

Fasted WT and *SSTR4*$^{-/-}$ mice ($n = 6$ for both WT and *SSTR4*$^{-/-}$ mice) were anaesthetized with diethyl ether and exsanguinated from the carotid artery. A ~15-cm-long segment of the ileum was dissected and placed in ice-cold aerated Krebs-Ringer solution (118.3 mM NaCl, 4.7 mM KCl, 1.2 mM $MgSO_4$, 1.2 mM KH_2PO_4, 2.5 mM $CaCl_2$, 25 mM $NaCHO_3$, 0.026 mM CaEDTA and 11.1 mM glucose). Smooth muscle strips were prepared as previously described [22]. Briefly, after opening the intestine along the mesenteric border, the mucosa was removed and smooth muscle strips were cut in the longitudinal direction. The strips were mounted in 5 ml organ baths filled with Krebs-Ringer solution (37°C, aerated with 5% CO_2 / 95% O_2) between two platinum ring electrodes (distance in between rings: 10 mm, diameter of rings: 3 mm) for electrical stimulation of the tissue. The

Table 1 Primary and secondary antisera used for immunocytochemistry

Primary antisera			
Antigen	**Host**	**Dilution**	**Source**
CGRP	Rabbit	1/5000	Sigma, St. Louis, MO, USA (C8198)
GFAP	Rabbit	1/500	DAKO, Glostrup, Denmark (Z0334)
mMCP-1	Rat	1/200	Prof. Dr. HRP Miller, Edinburgh, UK
nNOS	Rabbit	1/1000	EuroDiagnostica, Malmö, Sweden (B220–1)
PECAM-1	Goat	1/500	Santa Cruz Biotechnology, Santa Cruz, CA, USA (sc-1506)
PGP	Rabbit	1/1000	Biogenesis, Poole, UK (7863--2004)
S100	Rabbit	1/5000	DAKO (Z0311)
SOM	Rat	1/100	Biogenesis (8330--0009)
SSTR1	Rabbit	1/500	Biotrend, Köln, Germany (SS-840)
SSTR2A	Rabbit	1/2000	Biotrend (SS-800)
SSTR3	Rabbit	1/500	Biotrend (SS-850)
SSTR4	Rabbit	1/500	Sigma (S0945)
SSTR5	Rabbit	1/200	Abcam, Cambridge, UK (ab13121)
substance P	Rat	1/100	Biogenesis (8450–0505)

Secondary and tertiary antisera	**Dilution**	**Source**
Cy™-3-conjugated donkey anti-rabbit IgG	1/500	Jackson Immunoresearch, West Grove, PA, USA
Cy™-3-conjugated donkey anti-rat IgG	1/500	Jackson Immunoresearch
Cy™-5-conjugated Fab fragments of goat anti-rabbit IgG	1/400	Jackson Immunoresearch
FITC-conjugated goat anti-rat IgG	1/100	Jackson Immunoresearch
FITC-conjugated donkey anti-rabbit IgG	1/100	Jackson Immunoresearch
Biotinylated Fab fragments of goat anti-rabbit IgG	1/2000	Rockland, Gilbertsville, PA, USA
Biotin-conjugated tyramide signal amplification kit		PerkinElmer Life Sciences, Boston, MA, USA

PGP = protein gene product 9.5, nNOS = neuronal nitric oxide synthase, GFAP = glial fibrillary acidic protein, mMCP-1 = mouse mast cell protease-1, PECAM-1 = platelet/endothelial cell adhesion molecule.

lower end of the muscle strip was fixed and the other end connected to a strain gauge transducer (Scaime transducers, Annemasse, France) for recording of isometric tension. After a 30 min. equilibration period, the strips were contracted with 0.1 μM carbachol to obtain the optimal length-tension relationship. The tissues were allowed to equilibrate for 60 min. before starting the experimentation. During the equilibration period, the preparations were washed every 15 min. with fresh Krebs-Ringer solution.

Contractions of neurogenic origin were induced by electrical field stimulation (EFS) of enteric nerves. The frequency–response curves to EFS (0.25–8 Hz; pulse duration: 1 msec., pulse train: 10 sec.) were compared between ileal muscle strips from WT and *SSTR4*$^{-/-}$ mice. In a second series of experiments, concentration–response curves to the muscarinic receptor agonist carbachol (10–1000 nM), prostaglandin F2α (PGF-2α, 30–100 nM) and serotonin (10–30 nM) were constructed and compared between WT and *SSTR4*$^{-/-}$ smooth muscle strips.

Tissue preparation for immunocytochemistry, RT-PCR and qPCR

Non-infected and 8-week-old *S. mansoni*-infected (8w p.i.) *SSTR4*$^{-/-}$ mice (n = 8 for both groups) were killed by cervical dislocation and intestinal tissue was processed as described [1, 2]. Briefly, after flushing the ileum, three parts at the distal end (±5 mm each) were dissected. One part was used for cryosectioning, one for RNA isolation and the final one for paraffin embedding. The remaining portion was processed for whole-mount preparations. A few cryosections of each inflamed ileum were used to compare the inflammatory characteristics with previously described features [23]. Whole-mount preparations and cryosections were further processed for immunocytochemistry.

Immunocytochemistry and quantitative analyses

All immunocytochemical incubations were performed as previously described [1, 2]. Primary antibodies were diluted in 0.1 M PBS (pH 7.4) with 0.05% thimerosal (PBS‡), containing 10% normal horse serum (NHS) and 0.1% Triton X-100 (Table 1). Secondary and tertiary antibodies were diluted in PBS‡ containing 1% NHS. SSTRs were detected using the tyramide signal amplification (TSA) method following the manufacturer's guidelines (PerkinElmer Life Science, Boston, MA, USA). Whole-mount preparations and cryosections were pre-incubated in PBS‡ containing 5% bovine serum albumin, 10% NHS and 1% Triton X-100 for 30 min. and incubated with primary antibody for 16 hrs, followed by an appropriate secondary and/or tertiary antibody for 1 hr. In double and triple immunocytochemical procedures, cryosections and whole-mount preparations were subjected to additional conventional immunocytochemical stainings. Negative controls, in which the primary antibodies were omitted, and interference control

Table 2 5′→3′ sequence, annealing temperature of the qPCR primers and the temperature at which the fluorescence signal was measured

Primer	Sequence	T_A (°C)	T_M (°C)
CGRP-α forward primer	CATGGCCACTCTCAGTGA	64	82
CGRP-α reverse primer	GCTCCCTGGCTTTCATC		
CGRP-β forward primer	CCAGTCAAATATGATGGTGTCT	60	79
CGRP-β reverse primer	CATTGGCTGGATGGCTC		

Abbreviations: T_A = annealing temperature, T_M = fluorescence measurement temperature

stainings were performed [24]. The specificity of all antibodies was verified on murine brain sections by pre-absorption with the appropriate antigens (1 μg antigen per μg antibody). Quantitative analyses were performed on whole-mount preparations and/or cryosections to determine (*i*) the density of SOM- and SSTR2A-immunoreactive (ir) neurons, (*ii*) the percentage of SSTR2A-ir neurons containing neuronal nitric oxide synthase (nNOS), (*iii*) the density of SOM-ir endocrine epithelial cells and (*iv*) the density of mucosal mast cells (MMC) in 8w p.i. conditions. Detailed procedures of quantitative analyses were published previously [1, 2].

Immunocytochemical analysis of nerve fibre densities in whole-mount preparations

The density of enteric substance P-, CGRP- and SSTR1-ir nerve fibres was compared in whole-mount preparations of non-inflamed and 8w p.i. WT and *SSTR4*$^{-/-}$ ileum. For each image, a series of 27 consecutive 0.75-μm-thick confocal images, centred around the focal plane of the plexus, was taken at 25× magnification and projected into a single image. Ten randomly chosen, non-overlapping images were taken of each whole-mount preparation; three whole-mount preparations were analysed per animal. All images were captured using identical confocal settings. The fluorescent area of each image was measured with Cell P software (Olympus, London, UK) using identical threshold settings for all images. The total surface of each image was 136,384 μm^2. Results are expressed as the number of fluorescent pixels in thousands (representing the density of fluorescent nerve fibres) per mm^2 whole-mount preparation ± standard error.

RNA treatment

Total RNA of ileum and brain cortex was isolated using Trizol reagent (Life Technologies, Inc., Gaithersburg, MD, USA). Five micrograms of RNA were treated with the Turbo DNA-*free* kit (Ambion, Austin, TX, USA). One microgram of DNase-treated RNA was reverse-transcribed with the Transcriptor First Strand cDNA synthesis kit (Roche, Mannheim, Germany). The efficiency of the reverse transcription was verified using control RNA and primers included in the reverse transcription kit.

RT-PCR

DNase-treated RNA samples served as negative controls. Primer sequences for SSTRs and their amplification protocols were described previously [1]. RT-PCR experiments were performed on a MJ Mini Cycler (Biorad, Hercules, CA, USA) in a total reaction volume of 25 μl containing 1 μl cDNA, 0.4 μM forward and reverse primer and 12.5 μl HotstarTaq Master Mix (Qiagen, Hilden, Germany). Amplification products were separated on a 2% agarose gel and visualized under ultraviolet illumination.

qPCR

Primer sequences and amplification protocols for SOM, SSTRs and substance P were published previously [1, 25]. Primer characteristics for CGRP-α and CGRP-β are listed in Table 2. All reactions were performed in triplicate using the Lightcycler FastStart DNA Master^{PLUS} SYBR Green I kit (Roche) with fructosamine-3-kinase (F3K) and β-2-microglobulin (B2M) as reference genes [1].

Statistical analysis

Data on *in vivo* motility and *in vitro* contractility experiments were analysed by unpaired Student's t-test, data on quantitative analyses and qPCR by ANOVA followed by a Bonferroni *post hoc* test for comparison between different experimental groups. All data are expressed as means ± standard error of the mean. Significance was assumed at $P < 0.05$.

Results

Morphological and functional comparison of WT and *SSTR4*$^{-/-}$ ileum

Several morphological and functional characteristics of the *SSTR4*$^{-/-}$ ileum were compared to those of WT animals. In non-inflamed conditions, intestinal morphology, *in vivo* motility and *in vitro* intestinal smooth muscle contractility were compared between WT and *SSTR4*$^{-/-}$ mice. In view of the pivotal role of MMC in intestinal inflammatory pathologies and of the time- and space-dependent recruitment of these cells in the *S. mansoni*-infected murine ileum, inflammatory responses in WT and *SSTR4*$^{-/-}$ ileum were compared by investigating MMC densities and pathomorphological alterations in both mouse strains [26, 27].

In non-inflamed conditions, no morphological differences were observed in the structural organization of the WT and *SSTR4*$^{-/-}$ ileum (Fig. 1A and B). *In vivo* motility studies revealed no significant

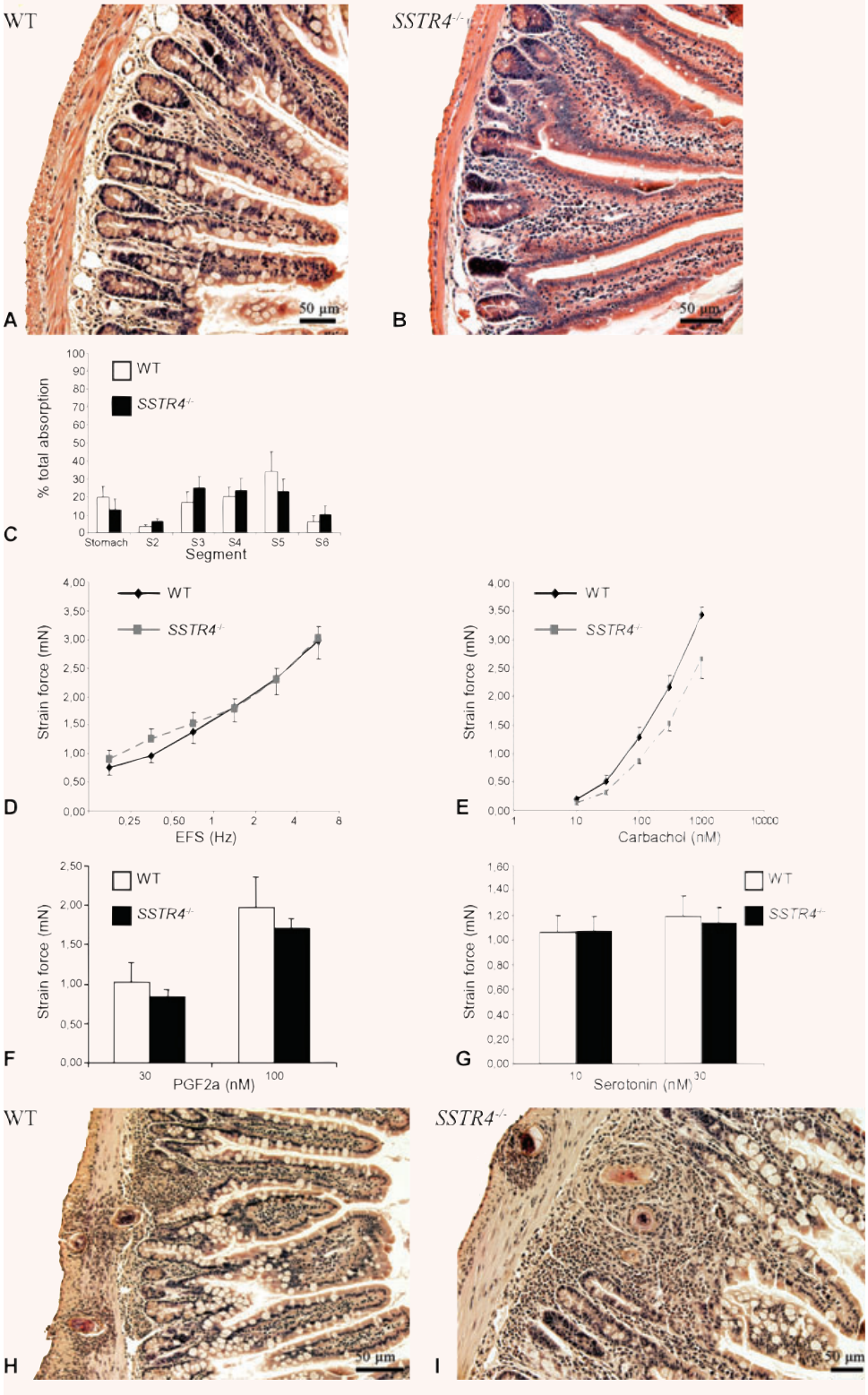

Fig. 1A, **B:** HE-stained paraffin-embedded light microscopic sections demonstrating the identical small intestinal morphology in WT (**A**) and *SSTR4*$^{-/-}$ (**B**) mice in non-inflamed conditions. (**C**) The global distribution of Evans blue in the different segments investigated in WT and *SSTR4*$^{-/-}$ mice. (**D**)–(**G**): *In vitro* contractility measurements of intestinal smooth muscle strips from non-infected WT and *SSTR4*$^{-/-}$ mice. The fr quency–response curve to EFS (**D**) and the concentration–response curve to carbachol (**E**) demonstrate similar responses in smooth muscle strips from both mouse strains. Also the evoked contractility responses to PGF-2α (**F**) and serotonin (**G**) are similar in WT and *SSTR4*$^{-/-}$ mice. **H–I**: HE-stained paraffin-embedded light microscopic sections demonstrating the appearance of intestinal granulomas, thickening of the tunica muscularis, broadening of the intestinal villi and disturbance of the architecture of the myenteric plexus in the 8w p.i. small intestine of WT (**H**) and *SSTR4*$^{-/-}$ (**I**) mice.

Table 3 Density of MMC in the 8w p.i. ileum of WT and *SSTR4*$^{-/-}$ mice. Densities are expressed as the number of MMC per mm³ ileum ± standard deviation. Data were analysed by unpaired Student's t-test.

	MMC density
Wild-type	51,978 ± 16,426
SSTR4$^{-/-}$	45,256 ± 7598

differences in intestinal transit (76 ± 7.3% in WT *versus* 76.1 ± 8.7% in *SSTR4*$^{-/-}$ mice, $P = 1$) or in the geometric centre (3.6 ± 0.4% in W *versus* 3.7 ± 0.3 in *SSTR4*$^{-/-}$ mice, $P = 0.9$) between WT and *SSTR4*$^{-/-}$ mice in physiological conditions. The global distribution of Evans blue in the different segments investigated in WT and *SSTR4*$^{-/-}$ mice is depicted in Fig. 1C. *In vitro* contractility experiments demonstrated that intestinal smooth muscle strips of WT and *SSTR4*$^{-/-}$ mice showed similar contractility responses to EFS, carbachol, PGF-2α and serotonin (Fig. 1D–G).

Intestinal schistosomiasis induced several morphological changes in the *SSTR4*$^{-/-}$ ileum (diffuse mucosal inflammation, the presence of numerous granulomas, thickening of the muscularis mucosa, broadening of the intestinal villi and disturbance of the architecture of the myenteric plexus) and is as such in accordance with the histopathological scoring seen in intestinal schistosomiasis in infected WT mice (Fig. 1H and I) [1, 23]. Comparison of MMC densities revealed the almost complete absence of MMC in the non-inflamed WT and *SSTR4*$^{-/-}$ mice ileum. Intestinal schistosomiasis induced a profound mastocytosis in the mucosal and submucosal layers of WT and *SSTR4*$^{-/-}$ mice, although no significant differences were observed between both mouse strains (Table 3).

Detection of SSTRs in non-inflamed and 8w p.i. *SSTR4*$^{-/-}$ ileum using RT-PCR

SSTR expression in the *SSTR4*$^{-/-}$ ileum was investigated with RT-PCR using brain tissue as a positive control (Fig. 2) [28, 29]. mRNA for SSTR1,2,3,5 was detected in both the non-inflamed and 8w p.i. *SSTR4*$^{-/-}$ ileum. The distribution of these receptors in *SSTR4*$^{-/-}$ ileum was further investigated by immunocytochemistry.

Immunocytochemistry

Interference control stainings, negative control stainings and preabsorption experiments demonstrated the specificity of all antibodies used and the lack of cross-reactivity amon antibodies used in different steps of the staining protocols. Paraffin-embedded coronal brain sections of WT mice showed immunoreactivity (IR) for all SSTRs as previously described [28, 29].

In cryosections of the non-inflamed *SSTR4*$^{-/-}$ ileum, SOM was detected in endocrine epithelial cells, in enteric neurons, in nerve fibres in the myenteric and submucous plexus and in nerve fibres

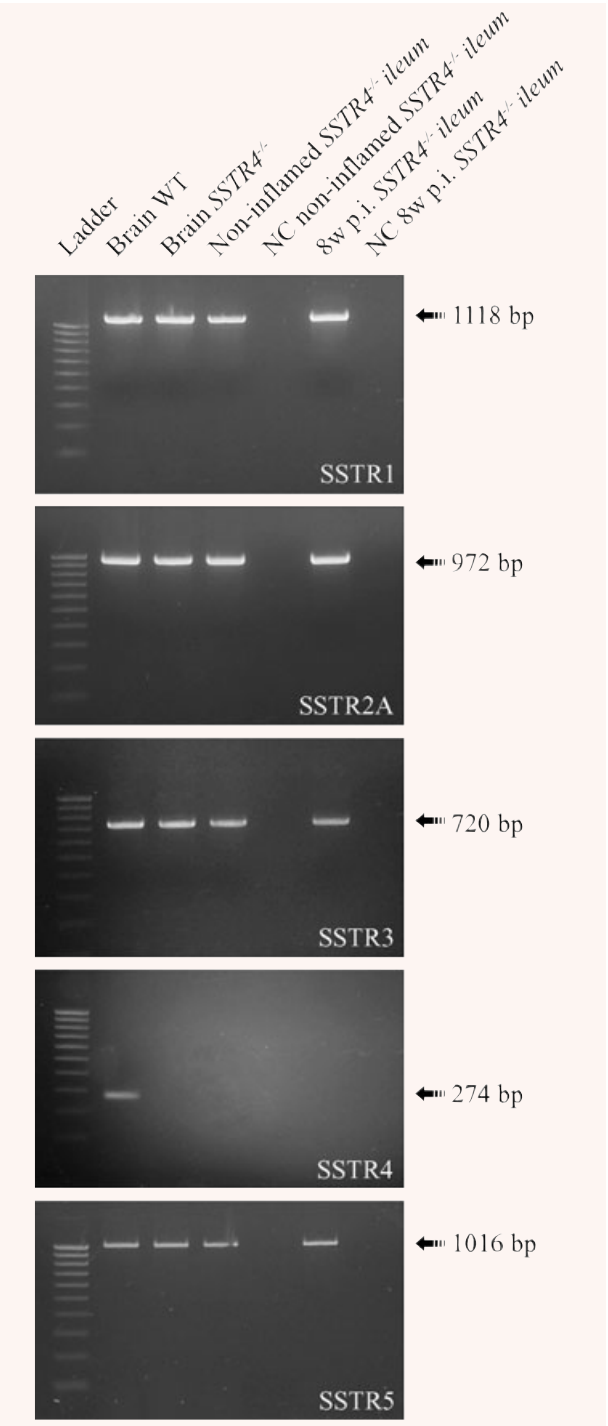

Fig. 2 RT-PCR experiments demonstrated the expression of SSTR1,2,3,5 in non-inflamed and in 8w p.i. *SSTR4*$^{-/-}$ ileum. Cortical brain cDNA samples of WT animals served as positive controls for SSTR expression. All SSTRs, except for SSTR4, were detected both in brain and in non-inflamed and 8w p.i. ileum of *SSTR4*$^{-/-}$ mice. NC = negative control, bp = basepairs

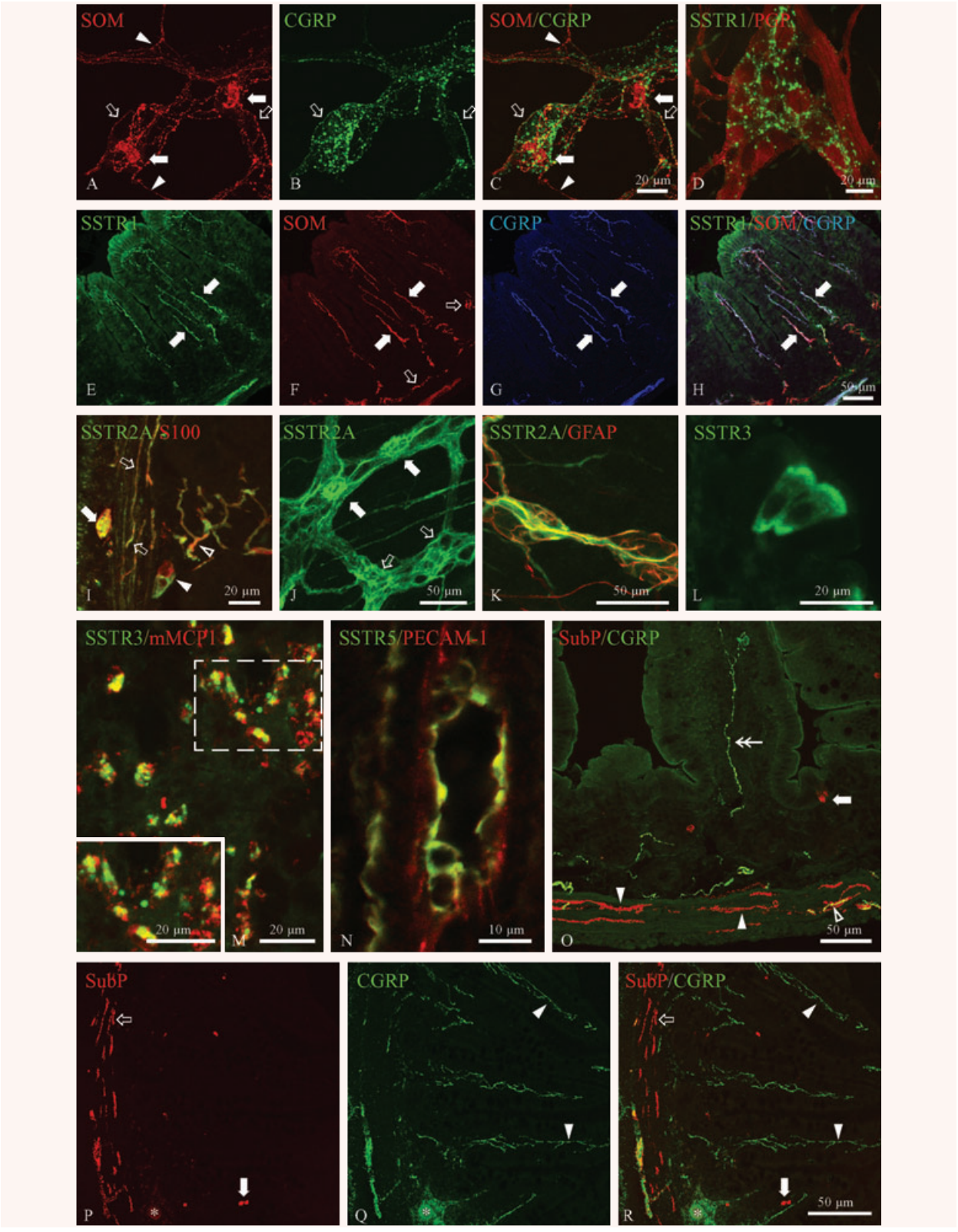

Fig. 3 Immunocytochemical detection of SSTRs and several peptides in the non-inflamed and 8w p.i. *SSTR4*$^{-/-}$ ileum. **A–C**: Whole-mount preparation of the non-inflamed *SSTR4*$^{-/-}$ myenteric plexus showing the expression of SOM in the soma of myenteric neurons (filled arrows) and in a vast network of SOM-ir nerve fibres, some of which co-express CGRP (hollow arrows). The arrowheads point towards SOM^{+}/CGRP^{-} nerve fibres. **D**: SSTR1 was detected in nerve fibres in myenteric whole-mount preparations of the non-inflamed *SSTR4*$^{-/-}$ ileum. **E–H**: Immunocytochemical triple staining for SSTR1, SOM and CGRP on cryosections of the non-inflamed *SSTR4*$^{-/-}$ ileum. All SSTR1-expressing nerve fibres in the lamina propria (filled arrows, **E**) also expressed SOM (**F**) and CGRP (**G**). The hollow arrows in F depict SOM-ir nerve fibres which do not express SSTR1 or CGRP. **I–K**: Immunofluorescent detection of SSTR2A in cryosections (**I**) and whole-mount preparations (**J**, **K**) of 8w p.i. *SSTR4*$^{-/-}$ ileum. **I**: Cryosections revealed SSTR2A expression in S100-labelled glial cells in the myenteric plexus (filled arrow), in the external muscle layers (hollow arrows), in the submucous plexus (filled arrowhead) and in the lamina propria (hollow arrowhead). **J**: SSTR2A expression in both myenteric neurons (filled arrows) and myenteric glial cells (hollow arrows). **K**: In the submucous plexus, SSTR2A was only detected in glial cells. **L**: SSTR3 immunoreactivity (IR) in epithelial cells at the top of the villi as detected in cryosections of non-inflamed *SSTR4*$^{-/-}$ ileum. **M**: In the 8w p.i. *SSTR4*$^{-/-}$ intestine, SSTR3 was observed in almost all mMCP1-labelled mucosal mast cells. The inset shows a higher magnification picture of the white dotted box. **N**: Endothelial cells of a small-diameter blood vessel in the submucosa, labelled by PECAM-1, showing SSTR5 IR. **O**: Cryosection of the non-inflamed *SSTR4*$^{-/-}$ ileum showing widespread distribution of substance P (SubP) and CGRP. Substance P was detected in nerve fibres at the base of the crypts and in the external muscle layers (filled and open arrowheads) and in endocrine cells (filled arrow). The nerve fibres indicated by the hollow arrow and the filled arrowheads did not co-express CGRP, whereas some nerve fibres in external muscle layers contained both substance P and CGRP (hollow arrowhead). The double arrow points to a CGRP^{+}/substance P^{-} nerve fibre in the lamina propria. **P-R**: Cryosection of the 8w p.i. *SSTR4*$^{-/-}$ ileum demonstrating substance P IR in endocrine cells (filled arrows) and in nerve fibres in the outer muscle layers (hollow arrow). The filled arrowheads show sprouting of CGRP-ir nerve fibres in the lamina propria. The parasite egg and the surrounding granuloma are indicated by asterisks.

Table 4 Percentage of SOM-ir enteric neurons in whole-mount preparations of non-inflamed and 8w p.i. WT and *SSTR4*$^{-/-}$ ileum. Results are expressed as the percentage of SOM-ir neurons in the enteric plexuses ± standard deviation.

	Non-inflamed	8w p.i.
Myenteric plexus		
WT	3.5 ± 0.9	4.1 ± 0.7
SSTR4$^{-/-}$	4.3 ± 0.5	6.9 ± 0.8*,‡
Submucous plexus		
WT	32.6 ± 7.3	34.1 ± 5.3
SSTR4$^{-/-}$	34.2 ± 2.3	34.3 ± 1.8

* = significantly different between WT and *SSTR4*$^{-/-}$ ileum ($P < 0.05$), ‡ = significantly different between non-inflamed and 8w p.i. conditions ($P < 0.05$).

Table 5 Density of SOM-ir endocrine epithelial cells in non-inflamed and 8w p.i. WT and *SSTR4*$^{-/-}$ ileum. Results are expressed as the number of SOM-ir endocrine epithelial cells per mm^3 terminal ileum ± standard deviation.

	Non-inflamed	8w p.i.
WT	3580 ± 540	810 ± 210‡
SSTR4$^{-/-}$	546 ± 185*,‡	201 ± 107*,‡

* = significantly different between WT and *SSTR4*$^{-/-}$ ileum ($P < 0.05$), ‡ = significantly different between non-inflamed and 8w p.i. conditions ($P < 0.05$).

running within the outer muscle layers, at the base of the crypts of Lieberkühn and in the lamina propria. Whole-mount preparations revealed SOM expression in individual neurons and in a vast network of nerve fibres in both enteric plexuses of the *SSTR4*$^{-/-}$ mice (Fig. 3A–C). The majority of these SOM-ir nerve fibres in whole-mount preparations did not co-express CGRP, indicative of their intrinsic origin [30]. A similar SOM distribution pattern was observed in cryosections of the 8w p.i. *SSTR4*$^{-/-}$ ileum, with additional sprouting of SOM-ir nerve fibres in the lamina propria and in the granulomas. The density of SOM-ir myenteric neurons did not differ between WT and *SSTR4*$^{-/-}$ mice in non-inflamed conditions. However, intestinal inflammation induced a significantly increased density of SOM-ir myenteric neurons in *SSTR4*$^{-/-}$ mice, whereas the density in WT animals remained unaltered (Table 4). In contrast, the density of SOM-ir endocrine epithelial cells in the *SSTR4*$^{-/-}$ ileum was dramatically reduced compared to WT animals, both in non-inflamed and in inflamed conditions (Table 5). However, intestinal inflammation decreased the density of SOM-ir endocrine cells in both WT and *SSTR4*$^{-/-}$ mice.

In the non-inflamed *SSTR4*$^{-/-}$ ileum, SSTR1 was detected in some epithelial cells at the base of the crypts of Lieberkühn and in nerve fibres at the base of the crypts, in both enteric plexuses (Fig. 3D) and in SOM- and CGRP-expressing nerve fibres in the lamina propria (Fig. 3E–H). All SSTR1-ir nerve fibres also expressed CGRP, demonstrating the exclusive presence of SSTR1 on extrinsic nerve fibres. The density of SSTR1-ir nerve fibres in the enteric plexuses was much higher in *SSTR4*$^{-/-}$ than in WT animals (Table 6). The 8w p.i. *SSTR4*$^{-/-}$ ileum was characterized by a similar SSTR1 distribution pattern, with additional expression of SSTR1 on almost all MMC and a strongly ramified network of SSTR1-ir nerve fibres in the lamina propria. As previously described in WT mice, the few MMC present in the non-inflamed *SSTR4*$^{-/-}$ ileum did not express SSTR1 [1].

SSTR2A IR was demonstrated in glial cells located in the lamina propria, at the base of the crypts of Lieberkühn and in the

Table 6 Density of different nerve fibre populations in whole mount preparations of both enteric plexuses in non-inflamed and 8w p.i. WT and *SSTR4*$^{-/-}$ ileum. Results are expressed as the number of fluorescent pixels in thousands per mm² whole-mount preparation ± standard deviation.

		Non-infected	8w p.i.
SSTR1	Myenteric plexus		
	WT	5.6 ± 2.0	27.6 ± 6.1‡
	SSTR4$^{-/-}$	10.4 ± 1.6*	88.5 ± 14.7*,‡
	Submucous plexus		
	WT type	1.9 ± 0.7	2.5 ± 0.7
	SSTR4$^{-/-}$	2.3 ± 1	4.3 ± 1.2*,‡
Substance P	Myenteric plexus		
	WT	62.6 ± 5.4	119.5 ± 13.5‡
	SSTR4$^{-/-}$	82.6 ± 9.6*	149 ± 14.3*,‡
	Submucous plexus		
	WT	24.4 ± 5.6	59.8 ± 8.6‡
	SSTR4$^{-/-}$	27.4 ± 6.3	84.6 ± 10.2*,‡
CGRP	Myenteric plexus		
	WT	10.3 ± 3	33.2 ± 3.6‡
	SSTR4$^{-/-}$	11.3 ± 2.3	43 ± 4.1*,‡
	Submucous plexus		
	WT	4.9 ± 1.5	10.6 ± 3.2‡
	SSTR4$^{-/-}$	4.3 ± 1.2	17.8 ± 3.7*,‡

* = significantly different between WT and *SSTR4*$^{-/-}$ ileum ($P < 0.05$), ‡ = significantly different between non-inflamed and 8w p.i. conditions ($P < 0.05$).

external muscle layers of both the non-inflamed and the 8w p.i. *SSTR4*$^{-/-}$ ileum (Fig. 3I). Immunofluorescent labelling of SSTR2A on whole-mount preparations of the myenteric plexus disclosed IR both in enteric Dogiel type I neurons and in glial cells (Fig. 3J), whereas only glial cells were labelled in the submucous plexus (Fig. 3K). The percentages of SSTR2A-ir myenteric neurons and nNOS-expressing SSTR2A-ir neurons did not differ between WT and *SSTR4*$^{-/-}$ mice, either in non-inflamed or in 8w p.i. conditions (Table 7).

Immunocytochemical detection of SSTR3 in the non-inflamed *SSTR4*$^{-/-}$ ileum revealed expression in a few epithelial cells at the base of the intestinal crypts and at the top of the villi (Fig. 3L). SSTR3-ir nerve fibres were occasionally observed at the base of the intestinal crypts and in the lamina propria of the non-inflamed small *SSTR4*$^{-/-}$ intestine. These SSTR3-ir nerve fibres, just like the SSTR1-positive fibres, also expressed SOM and CGRP. In the 8w p.i. *SSTR4*$^{-/-}$ ileum, SSTR3 was regularly detected in SOM- and CGRP-expressing nerve fibres in the lamina propria and in almost all MMC (Fig. 3M).

SSTR5 was expressed in endothelial cells of small- and medium-diameter blood vessels in *SSTR4*$^{-/-}$ ileum, mainly in the submucosa and the lamina propria (Fig. 3N), both in non-inflamed and in 8w p.i. conditions.

Because SSTR4 has been shown to suppress the neuronal release of substance P and CGRP, we compared the distribution of these proteins in the small intestine of WT and *SSTR4*$^{-/-}$ mice. In the non-inflamed intestine of both mouse strains, substance P was detected in endocrine epithelial cells and in nerve fibres in the lamina propria, at the base of the intestinal crypts, in the myenteric and the submucous plexus and in the outer muscle layers (Fig. 3O). Most of these nerve fibres in the lamina propria and the submucosa also expressed CGRP. CGRP was additionally expressed in nerve fibres in both enteric plexuses and in the lamina propria. Quantitative analysis revealed a higher density of substance P-ir nerve fibres in the myenteric plexus of *SSTR4*$^{-/-}$ than in that of WT mice (Table 6).

In both WT and *SSTR4*$^{-/-}$ mice, intestinal inflammation induced sprouting of CGRP-ir nerve fibres in the lamina propria and the submucosa, and of substance P-ir nerve fibres in the immediate environment of the granulomas in the muscle layers (Fig. 3P–R). Moreover, densities of CGRP- and substance P-ir nerve fibres in both enteric plexuses were two- to threefold higher in 8w p.i. than in non-inflamed ileum in both WT and *SSTR4*$^{-/-}$ mice (Table 6, Fig. 4A–D). However, in the 8w p.i. conditions, the networks of enteric CGRP- and substance P-ir nerve fibres were more dense in *SSTR4*$^{-/-}$ than in WT mice. Apart from the increased densities of substance P- and CGRP-ir nerve fibres in the enteric plexuses, no morphological differences in the distribution of substance P or CGRP were observed between WT and *SSTR4*$^{-/-}$ mice.

qPCR

Genetic depletion of *SSTR4* was accompanied by compensatory changes in the mRNA levels of the other SSTRs (Fig. 4E). mRNA levels for all four other SSTR subtypes were significantly higher in the *SSTR4*$^{-/-}$ ileum than in the WT ileum, both in non-inflamed and 8w p.i. conditions. Intestinal inflammation significantly elevated SSTR1 and SSTR3 mRNA levels in WT and *SSTR4*$^{-/-}$ mice. In contrast to WT mice, SSTR2A mRNA levels in the 8w p.i. *SSTR4*$^{-/-}$ ileum were reduced compared to non-inflamed conditions, whereas intestinal inflammation did not change SSTR5 mRNA levels in *SSTR4*$^{-/-}$ ileum.

SOM, CGRP-α, CGRP-β and substance P mRNA levels were also quantified (Fig. 4F). In the non-inflamed *SSTR4*$^{-/-}$ ileum, SOM and substance P mRNA levels were elevated compared to the non-inflamed WT ileum, whereas no significant changes in CGRP-α or CGRP-β mRNA were detected. Both in WT and *SSTR4*$^{-/-}$ mice, intestinal inflammation induced significantly increased mRNA levels for all peptides investigated, although mRNA levels for all four peptides were significantly higher in inflamed *SSTR4*$^{-/-}$ than in inflamed WT animals.

Discussion

In sharp contrast to the complete absence of compensatory effects in the small intestine of *SSTR2*$^{-/-}$ mice, in terms of up- or

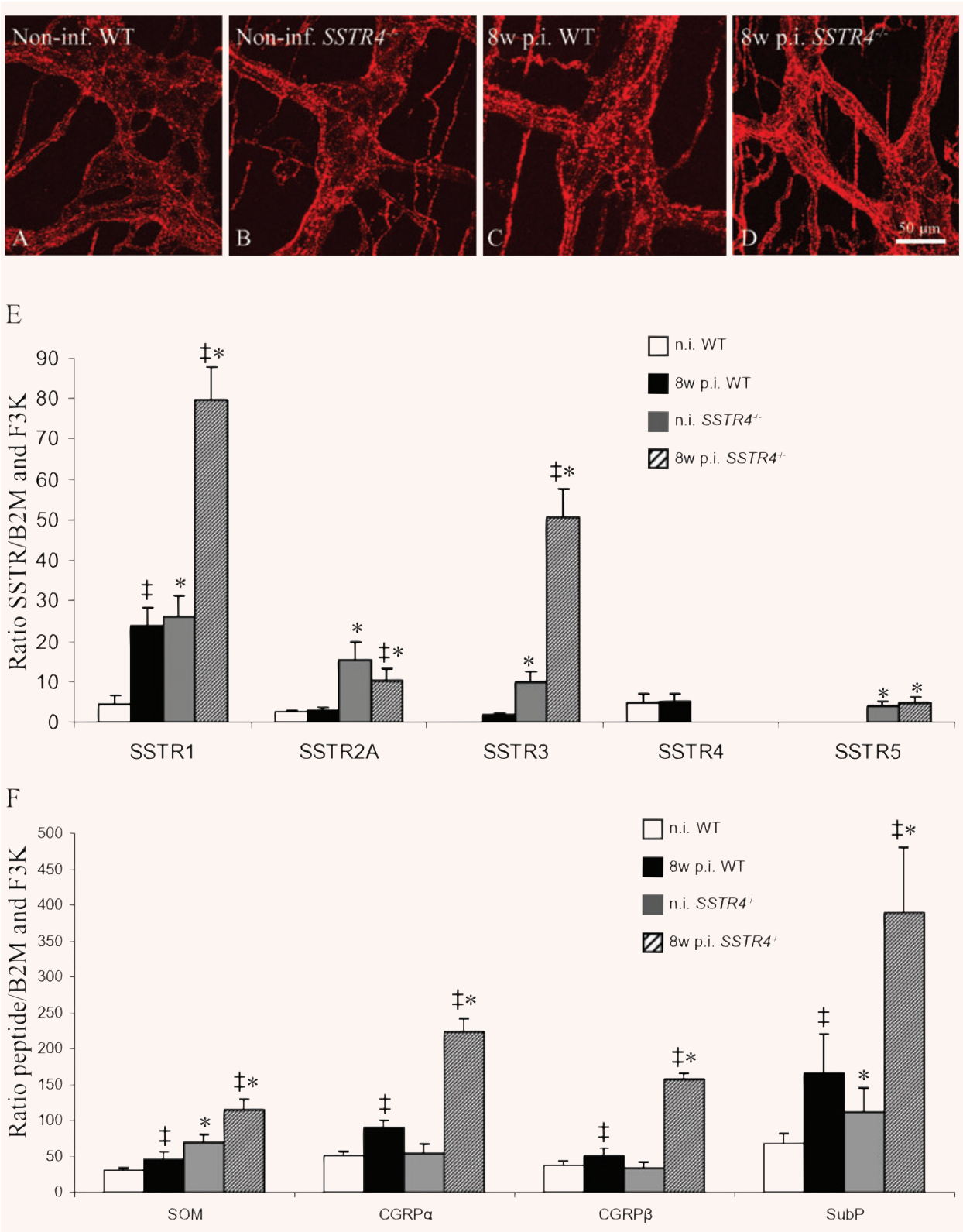

Table 7 Percentages of SSTR2A-ir (A) and nNOS-expressing SSTR2A-ir (B) myenteric neurons in whole-mount preparations of the non-inflamed and 8w p.i. WT and *SSTR4*$^{-/-}$ ileum

	A		B	
	Non-inflamed	**8w p.i.**	**Non-inflamed**	**8w p.i.**
WT	4.98 ± 0.7	5.67 ± 0.59	68.7 ± 3.6	69.66 ± 2.1
SSTR4$^{-/-}$	5.21 ± 0.59	5.54 ± 0.72	71.2 ± 4.1	72.3 ± 2.9

Section A of the table shows the percentages of SSTR2A-ir myenteric neurons in proportion to the total number of myenteric neurons. Section B of the table shows the percentages of SSTR2A-ir myenteric neurons containing nNOS. Results are expressed as means ± standard deviation.

down-regulation of other SSTRs, the *SSTR4*$^{-/-}$ ileum does show significant changes both in the distribution pattern and in the expression levels of several neuropeptides and SSTR subtypes [2].

Focussing on the altered expression of SSTRs in the small intestine of *SSTR4*$^{-/-}$ mice, several of these compensatory effects relate to the neuronal expression of SSTRs. As previously demonstrated in WT animals, all SSTR1-ir nerve fibres in the *SSTR4*$^{-/-}$ ileum derive from extrinsic afferent neurons [1]. Therefore, the increased density of SSTR1-ir nerve fibres in *SSTR4*$^{-/-}$ ileum suggests that genetic depletion of SSTR4 affects the extrinsic afferent innervation of the small intestine. As all SSTR1-containing nerve fibres were found to co-stain for SOM in the *SSTR4*$^{-/-}$ ileum, also the somatostatinergic component of the extrinsic innervation was altered in *SSTR4*$^{-/-}$ mice. The observations that SSTR2A is expressed in glial cells in both enteric plexuses in the *SSTR4*$^{-/-}$ ileum, but not in the myenteric plexus of WT animals, and that SSTR3 is clearly expressed in extrinsic nerve fibres in non-inflamed *SSTR4*$^{-/-}$ ileum, add further proof to the changed neuronal SSTR expression patterns and to the presence of distinct phenotypes within the enteric glial cell population in *SSTR4*$^{-/-}$ mice.

SSTR expression was also changed in non-neuronal intestinal cell types. For instance, SSTR5, which was not detected in WT ileum, was found in endothelial cells in the non-inflamed and 8w p.i. *SSTR4*$^{-/-}$ ileum, which is in line with the SSTR5 expression in human endothelial cells [31, 32]. These data indicate that SSTR4 is involved in the regulation of SSTR expression in the murine small intestine, both in neuronal and in non-neuronal cell types, although the precise mechanisms remain unclear.

Also the expression of SOM itself was markedly different in *SSTR4*$^{-/-}$ mice. SOM mRNA levels were higher in *SSTR4*$^{-/-}$ than in WT ileum, both in non-inflamed and in 8w p.i. conditions. In contrast to WT and *SSTR2*$^{-/-}$ mice, SOM IR was observed in a strongly ramified network of nerve fibres in the myenteric plexus of *SSTR4*$^{-/-}$ mice, possibly contributing to the increased SOM mRNA levels in *SSTR4*$^{-/-}$ ileum [1, 2]. Most of these SOM-ir nerve fibres are CGRP-immunonegative and most probably belong to the intrinsic SOM-ir somata, implying that the absence of SSTR4 also affects the intrinsic intestinal innervation [30]. However, as also the density of SSTR1- and SOM-expressing extrinsic nerve fibres in the *SSTR4*$^{-/-}$ ileum is strongly increased compared to WT tissue, it is hard to predict to what extent the extrinsic and intrinsic somatostatinergic innervation contribute to the increased SOM mRNA levels in *SSTR4*$^{-/-}$ ileum.

Despite these significant compensatory effects related to SOM and SSTRs, small intestinal morphology, motility and smooth muscle contractility to EFS, carbachol, PGF-2α and serotonin did not differ between WT and *SSTR4*$^{-/-}$ ileum in non-inflamed conditions. Therefore, SSTR4 does not seem to directly modulate intestinal motility in physiological conditions. The similar MMC densities and morphological appearance of the 8w p.i. WT and *SSTR4*$^{-/-}$ ileum indicate that SSTR4 is not directly involved in the mastocytosis or the morphological pathological characteristics of intestinal schistosomiasis.

Intestinal inflammation strongly reduced the density of SOM-expressing endocrine cells in WT and *SSTR4*$^{-/-}$ ileum. These findings are in line with repeatedly reported decreased densities of

Fig. 4 A–D: Comparison of the density of substance P-ir nerve fibres in the myenteric plexus of non-infected WT (A), non-infected *SSTR4*$^{-/-}$ (B), 8w p.i. WT (C) and 8w p.i. *SSTR4*$^{-/-}$ mice (D). **C–D:** Quantification of the mRNA levels for SSTRs, SOM, CGRP-α, CGRP-β and substance P in non-inflamed and 8w p.i. WT and *SSTR4*$^{-/-}$ ileum. **C**: In non-inflamed conditions, mRNA levels for all SSTRs were significantly increased in *SSTR4*$^{-/-}$ ileum compared to WT intestine. In WT mice, intestinal inflammation induced increased mRNA levels for all SSTRs. In *SSTR4*$^{-/-}$ mice, the same phenomenon was observed, except for SSTR2A mRNA levels, which were decreased compared to non-inflamed conditions. Moreover, except for SSTR2A, mRNA levels for all SSTRs were higher in 8w p.i. *SSTR4*$^{-/-}$ ileum than in 8w p.i. WT tissue. **D**: In non-inflamed conditions, mRNA levels for SOM and substance P were significantly higher in *SSTR4*$^{-/-}$ than in WT ileum, whereas no differences for CGRP-α or CGRP-β were detected. Intestinal inflammation was characterized by increased mRNA levels for all peptides investigated in the small intestine of both mouse strains. Moreover, mRNA levels for SOM, CGRP-α, CGRP-β and substance P were significantly increased in 8w p.i. *SSTR4*$^{-/-}$ ileum compared to 8w p.i. WT intestine. ‡ statistically significant difference between non-inflamed and 8w p.i. conditions ($P < 0.05$), * statistically significant difference between WT and *SSTR4*$^{-/-}$ ileum ($P < 0.05$)

SOM-ir endocrine epithelial cells in the bowel of patients with Crohn's disease and ulcerative colitis [33–35]. The density of SOM-ir endocrine epithelial cells was significantly decreased in *SSTR4*$^{-/-}$ ileum compared to WT intestine, both in non-inflamed and in 8w p.i. conditions, although the precise underlying mechanism is currently unknown.

SSTR4-selective agonists have been described to suppress the release of substance P and CGRP from primary afferents [15–17]. Our finding that the expression of substance P and both isoforms of CGRP is significantly increased in *SSTR4*$^{-/-}$ ileum, suggests that SSTR4 not only inhibits the neuronal release of these peptides, but also that this receptor modulates the neuronal expression of substance P and CGRP. Quantitative analyses indicate that the increased densities of substance P- and CGRP-ir enteric nerve fibres probably contribute to these enhanced expression levels of both neuropeptides. These data, combined with the similar MMC densities and morphological characteristics in the 8w p.i. WT and *SSTR4*$^{-/-}$ ileum, confirm the hypothesis that suppressing the pro-inflammatory activity of sensory neurons provides an important mechanism through which SSTR4 reduces inflammatory reactions and nociception in the GIT [36].

The combination of our morphological, molecular biological and quantitative data suggests that the small intestine of *SSTR4*$^{-/-}$ mice is characterized by significant alterations in both the expression and distribution pattern of SOM, SSTRs and the pro-inflammatory peptides substance P and CGRP. These data are in sharp contrast to the lack of compensatory effects in the small intestine of *SSTR2*$^{-/-}$ mice [2]. However, the precise mechanisms through which SSTR4 modulates GI activity and SSTR expression require further investigation. Therefore, it is concluded that in the GIT, SSTR4 is involved in the regulation of the neuronal expression of both pro- and anti-inflammatory peptides.

Acknowledgements

The authors thank the technical staff of the laboratories involved for their excellent technical assistance. This study was funded by the Interuniversity Attraction Pole (IUAP) project P5/20, a grant of the Institute for Scientific Research (FWO G.0377.04) and a fellowship from the Flemish Government to Joeri van Op den bosch (SB53449).

References

1. **Van Op den bosch J, Van Nassauw L, Lantermann K, *et al.*** Effect of intestinal inflammation on the cell-specific expression of somatostatin receptor subtypes in the murine ileum. *Neurogastroenterol Motil.* 2007; 19: 596–606.
2. **Van Op den bosch J, Lantermann K, Torfs P, *et al.*** Distribution and expression levels of somatostatin and somatostatin receptors in the ileum of normal and acutely Schistosoma mansoni-infected SSTR2 knockout/lacZ knockin mice. *Neurogastroenterol Motil.* 2008; 20: 798–807.
3. **Abdu F, Hicks GA, Hennig G, *et al.*** Somatostatin sst2 receptors inhibit peristalsis in the rat and mouse jejunum. *Am J Physiol Gastrointest Liver Physiol.* 2002; 282: G624–33.
4. **Van Hagen PM, Krenning PM, Kwekkeboom DJ, *et al.*** Somatostatin and the immune and hematopoetic system: a review. *Eur J Clin Invest.* 1994; 24: 91–9.
5. **Elliot DE, Li J, Blum AM, *et al.*** SSTR2A is the dominant somatosttain receptor subtype expressed by inflammatory cells, is widely expressed and directly regulates T cell IFN-gamma release. *Eur J Immunol.* 1999; 29: 2454–63.
6. **Scicchitano R, Dazin P, Bienenstock J, *et al.*** The murine IgA-secreting plasmacytoma MOPC-315 expresses somatostatin receptors. *J Immunol.* 1988; 141: 937–41.
7. **Chowers Y, Cahalon L, Lahav M, *et al.*** Somatostatin through its specific receptor inhibits spontaneous and TNF-α – and bacteria-induced IL-8 and IL-1β secretion from intestinal epithelial cells. *J Immunol.* 2000; 165: 2955–61.
8. **Kashiba H, Ueda Y, Senba E.** Coexpression of preprotachykinin-A, alpha-calcitonin gene- related peptide, somatostatin, and neurotrophin receptor family messenger RNAs in rat dorsal root ganglion neurons. *Neuroscience.* 1996; 70: 179–89.
9. **Hökfelt T, Elde R, Johansson O, *et al.*** Immunohistochemical evidence for separate populations of somatostatin-containing and substance P-containing primary afferent neurons in the rat. *Neuroscience.* 1976; 1: 131–6.
10. **Pintér E, Szolcsanyi J.** Inflammatory and antiinflammatory effects of antidromic stimulation of dorsal roots in the rat. *Agents Actions.* 1988; 25: 240–2.
11. **Carlton SM, Du J, Davidson E, *et al.*** Somatostatin receptors on peripheral primary afferent terminals: inhibition of sensitized nociceptors. *Pain.* 2001a; 90: 233–44.
12. **Carlton SM, Du J, Shengtai Z, *et al.*** Tonic control of peripheral cutaneous nociceptors by somatostatin receptors. *J Neurosci.* 2001b; 21: 4042–9.
13. **Helyes Z, Szabo A, Nemeth J, *et al.*** Antiinflammatory and analgesic effects of somatostatin released from capsaicin-sensitive sensory nerve terminals in a Freund's adjuvant-induced chronic arthritis model in the rat. *Arthritis Rheum.* 2004; 50: 1677–85.
14. **Heppelmann B, Pawlak M.** Peripheral application of cyclo-somatostatin, a somatostatin antagonist, increases the mechanosensitivity of rat knee joint afferents. *Neurosci Lett.* 1999; 259: 62–4.
15. **Elekes K, Helyes Z, Keresekai L, *et al.*** Inhibitory effects of synthetic somatostatin receptor subtype 4 agonists on acute and chronic airway inflammation and hyperreactivity in the mouse. *Eur J Pharmacol.* 2008; 578: 313–22.
16. **Helyes Z, Pintér E, Nemeth J, *et al.*** Anti-inflammatory effect of synthetic somatostatin analogues in the rat. *Br J Pharmacol.* 2001; 134: 1571–9.
17. **Pintér E, Helyes Z, Nemeth J, *et al.*** Pharmacological characterisation of the somatostatin analogue TT-232: effects on neurogenic and non-neurogenic inflammation and neuropathic hyperalgesia. *Naunyn-Schmiedeberg's Arch Pharmacol.* 2002; 366: 142–50.
18. **Videau C, Hochgeschwender U, Kreienkamp HJ, *et al.*** Characterisation of [125I]-Tyr0Trp8-somatostatin binding in

sst1- to sst4- and SRIF-gene-invalidated mouse brain. *Naunyn Schmiedebergs Arch Pharmacol.* 2003; 376: 562–571.

19. **Qiu C, Zeyda T, Johnson B, *et al.*** Somatostatin receptor subtype 4 couples to the M-current to regulate seizures. *J Neurosci.* 2008; 28: 3567–76.
20. **Smithers SR, Terry RJ.** Infection of laboratory hosts with cercariae of Schistosoma mansoni and the recovery of the adult worms. *Parasitology.* 1965; 55: 695–700.
21. **Seerden TC, De Winter BY, Van Den Bossche RM, *et al.*** Regional differences in gastrointestinal motility disturbances during acute necrotising pancreatitis. *Neurogastroenterol Motil.* 2005; 17: 671–9.
22. **De Man JG, De Winter BY, Seerden TC, *et al.*** Functional evidence that ATP or a related purine is an inhibitory NANC neurotransmitter in the mouse jejunum: study on the identity of P2X and P2Y purinoceptors involved. *Br J Pharmacol.* 2003; 140: 1108–16.
23. **Bogers JP, Moreels T, De Man J, *et al.*** Schistosoma mansoni infection causing diffuse enteric inflammation and damage of the enteric nervous system in the mouse small intestine. *Neurogastroenterol Motil.* 2000; 12:431–40.
24. **Shindler KS, Roth KA.** Double imunofluorescent staining using two unconjugated primary antisera raised in the same species. *J Histochem Cytochem.* 1996; 44: 1331–5.
25. **Colebrooke RE, Chan PM, Lynch PJ, *et al.*** Differential gene expression in the striatum of mice with very low expression of the vesicular monoamine transporter type 2 gene. *Brain Res.* 2007; 1152: 10–6.
26. **De Jonge F, Van Nassauw L, Van Meir F, *et al.*** Temporal distribution of distinct mast cell phenotypes during intestinal schistosomiasis in mice. *Parasite Immunol.* 2002; 24: 225–31.
27. **Wood JD.** Enteric neuroimmunophysiology and pathophysiology. *Gastroenterology.* 2004; 127: 635–57.
28. **Ramirez JL, Grant M, Norman M, *et al.*** Deficiency of somatostatin (SST) receptor type 5 (SSTR5) is associated with sexually dimorphic changes in the expression of SST and SST receptors in brain and pancreas. *Mol Cell Endocrinol.* 2004; 221: 105–19.
29. **Ramirez JL, Mouchantaf R, Kumar U, *et al.*** Brain somatostatin receptors are upregulated in the somatostatin-deficient mice. *Mol Endocrinol.* 2002; 16: 1951–63.
30. **De Jonge F, Van Nassauw L, Adriaensen D, *et al.*** Effect of intestinal inflammation on capsaicin-sensitive afferents in the ileum of *Schistosoma mansoni*-infected mice. *Histochem Cell Biol.* 2003; 119: 477–84.
31. **Adams RL, Adams IP, Lindow SW, *et al.*** Somatostatin receptors 2 and 5 are preferentially expressed in proliferating endothelium. *Br J Cancer.* 2005; 92: 1493–8.
32. **Yan S, Li M, Chai H, *et al.*** TNF-alpha decreases expression of somatostatin, somatostatin receptors and cortistatin in human coronary endothelial cells. *J Surg Res.* 2005; 123: 294–301.
33. **Koch TR, Carney JA, Morris VA, *et al.*** Somatostatin in the idiopathic inflammatory bowel diseases. *Dis Colon Rectum.* 1988; 31: 198–203.
34. **Calam J, Ghatei MA, Domin J, *et al.*** Regional differences in concentrations of regulatory peptides in human colon mucosal biopsy. *Dig Dis Sci.* 1989; 34: 1193–8.
35. **Watanabe T, Kubota Y, Sawada T, *et al.*** Distribution and quantification of somatostatin in inflammatory disease. *Dis Colon Rectum.* 1992; 35: 488–94.
36. **Pintér E, Helyes Z, Szolcsanyi J.** Inhibitory effect of somatostatin on inflammation and nociception. *Pharmacol Ther.* 2006; 112: 440–56.